PERGAMON

Central and South America

Atmospheric Environment 35 (2001) 1773–1781

ATMOSPHERIC ENVIRONMENT

www.elsevier.com/locate/atmosenv

Biomass burning losses of carbon estimated from ecosystem modeling and satellite data analysis for the Brazilian Amazon region

Christopher Potter[a,*], Vanessa Brooks Genovese[b], Steven Klooster[c], Matthew Bobo[b], Alicia Torregrosa[c]

[a]*Ecosystem Science and Technology Branch, NASA Ames Research Center, Moffett Field, CA 94035, USA*
[b]*Johnson Controls World Services, NASA Ames Operations, Moffett Field, CA 94035, USA*
[c]*California State University Monterey Bay, Seaside, CA 93955, USA*

Received 13 June 2000; received in revised form 20 August 2000; accepted 23 August 2000

Abstract

To produce a new daily record of gross carbon emissions from biomass burning events and post-burning decomposition fluxes in the states of the Brazilian Legal Amazon (Instituto Brasileiro de Geografia e Estatistica (IBGE), 1991. Anuario Estatistico do Brasil, Vol. 51. Rio de Janeiro, Brazil pp. 1–1024). We have used vegetation greenness estimates from satellite images as inputs to a terrestrial ecosystem production model. This carbon allocation model generates new estimates of regional aboveground vegetation biomass at 8-km resolution. The modeled biomass product is then combined for the first time with fire pixel counts from the advanced very high-resolution radiometer (AVHRR) to overlay regional burning activities in the Amazon. Results from our analysis indicate that carbon emission estimates from annual region-wide sources of deforestation and biomass burning in the early 1990s are apparently three to five times higher than reported in previous studies for the Brazilian Legal Amazon (Houghton et al., 2000. Nature 403, 301–304; Fearnside, 1997. Climatic Change 35, 321–360), i.e., studies which implied that the Legal Amazon region tends toward a net-zero annual source of terrestrial carbon. In contrast, our analysis implies that the total source fluxes over the entire Legal Amazon region range from 0.2 to 1.2 Pg C yr^{-1}, depending strongly on annual rainfall patterns. The reasons for our higher burning emission estimates are (1) use of combustion fractions typically measured during Amazon forest burning events for computing carbon losses, (2) more detailed geographic distribution of vegetation biomass and daily fire activity for the region, and (3) inclusion of fire effects in extensive areas of the Legal Amazon covered by open woodland, secondary forests, savanna, and pasture vegetation. The total area of rainforest estimated annually to be deforested did not differ substantially among the previous analyses cited and our own. Published by Elsevier Science Ltd.

1. Introduction

Among the major components necessary for understanding air pollution impacts on global climate, few are as uncertain as the rates of tropical biomass burning fluxes of trace gases and emission of smoke aerosols to the atmosphere. The humid tropics have been identified as a probable net source of carbon to the atmosphere, chiefly because of high deforestation rates and frequency of biomass burning (Ciais et al., 1995; Potter, 1999). The added effects of smoke emissions from forest fires on radiation fluxes, cloud microstructure, rainfall, and ozone sources are of major concern on regional and global scales (Kaufman et al., 1998).

We have generated new predictions of biomass accumulation in terrestrial ecosystems of the Brazilian

* Corresponding author. Tel.: +1-650-604-6164; fax +1-650-604-4680.
E-mail address: cpotter@gaia.arc.nasa.gov (C. Potter).

1352-2310/01/$ - see front matter. Published by Elsevier Science Ltd.
PII: S1352-2310(00)00459-3

Amazon using the NASA–CASA (Carnegie–Ames–Stanford Approach) model, which can be scaled up to regional levels using satellite data inputs (Potter and Klooster, 1997, 1999b; Potter, 1999). The model includes interactions of several key controls on net ecosystem production (NEP) of carbon and total biomass in the tropics: surface radiation fluxes, evapotranspiration and soil water balance, soil fertility, and microbial activity affecting decomposition of plant residues. Regional scaling is accomplished by merging input data sets from AVHRR, surface climate, radiation, vegetation, and soils with model algorithms for carbon and moisture flow and energy use processes in terrestrial ecosystems. Global satellite observations to drive the NASA–CASA model are an important feature for improving current carbon accounting, because (i) predicted carbon input fluxes into plants are formulated to be consistent with the range of measured rates from field studies worldwide, and (ii) actual regional patterns for land cover attributes, such as biomass of forests, may differ substantially from potential vegetation maps or from extrapolation using a small set of sparsely distributed site measurements.

2. Biomass modeling methods

A complete description of the previous NASA–CASA model design for regional carbon cycling in Amazon ecosystems is provided by Potter et al. (1998), including the method to estimate net primary production (NPP) as a product of cloud-corrected solar surface irradiance (S), fractional intercepted photosynthetically active radiation (FPAR) and a maximum light use efficiency term (ε), modified by normalized temperature (T) and moisture (W) stress scalars (Eq. (1)).

$$\mathrm{NPP} = S\ \mathrm{FPAR}\ \varepsilon T W. \quad (1)$$

In the regional simulation mode, estimation of FPAR comes from a vegetation index derived from AVHRR channel 1 (0.5–0.68 μm; visible) and channel 2 (0.73–1.1 μm; near-IR) reflectance values (Potter et al., 1993; Sellers et al., 1994). The W stress term is computed on the basis of the predicted monthly ratio of estimated evapotranspiration (EET) to potential evapotranspiration (PET; Priestly and Taylor, 1972).

Regional data sets (8-km resolution) from a geographic information system (GIS) are used as model drivers and land surface parameter files. We assembled a complete set of co-registered GIS raster coverages to serve as model-compatible inputs, including interpolated monthly (1982–1990) rainfall records from Brazil's Departamento Nacional de Aguas e Energia Eletrica (DNAEE) network, surface air temperature (New et al., 2000), surface solar radiation (from the International Satellite Cloud Climatology Program; Bishop and Rossow, 1991), soil type and texture (RADAMBRASIL; MME, 1981; Potter et al., 1998), land cover type (from AVHRR and Landsat classification; Stone et al. (1994)), and NASA AVHRR Pathfinder satellite vegetation index (Agbu and James, 1994) for the country of Brazil and, in some cases, for the larger Amazon region. Due to cloud cover and smoke-aerosol interference, which can be prevalent at different times and locations in the Amazon region, we applied Fourier smoothing algorithms (FA) developed by Los et al. (1994) for AVHRR data sets to further remove erroneousness atmospheric signals in the satellite greenness index. Application of the FA algorithm modified mean annual index values by more than +10% of their original values in approximately four out of every ten grid cells in the region (Potter et al., 1998).

Our aboveground biomass estimation methods do not derive directly from optical remote sensing (e.g., the AVHRR), but are based rather on multi-year inputs of NPP from satellite data using well-accepted methods previously described (Potter et al., 1993; Sellers et al., 1994). Biomass is subsequently estimated as a function of residence times and allocation rates in our ecosystem simulation model. Carbon and nitrogen allocation among leaf, wood, and fine root tissues from NPP (Table 1) are defined as a set of fractional allocation constants of plant tissue pools (α), and the mean residence time (τ, in years) of carbon in the standing plant tissue pools (Potter and Klooster, 1999a; Terborgh et al., 1997). Soil fertility effects are included in this model version to adjust these allocation constants for generalized nutrient limitations. We classified soil types in the Soil Map of Brazil (MME, 1981) according to three relative levels of soil fertility (low, medium, and high). On low fertility soils, an adjustment (+10%) is favored that allocates increasing root biomass for the acquisition of soil nutrients (Wilson and Tilman, 1991). On medium-to-high fertility soils, a similar adjustment is favored that allocates 10% more to above ground wood and leaf biomass for light harvesting functions in the canopy (Gleeson and Tilman, 1990; Redente et al., 1992; Lusk et al., 1997).

Following an initialization period of 100 years that equilibrated predicted carbon pools, we ran our model for nine successive years using the Brazil GIS data drivers beginning from 1981–1982 conditions. NASA–CASA results for total amounts of aboveground wood and leaf biomass across the Legal Amazon region for the early 1990s are 57.7 Pg (10^{15} g) wood C and 2.2 pg leaf C. The geographic distribution of NASA–CASA model forest biomass indicates that carbon amounts are highest in the seasonally dry forest areas of the eastern and southern states of Pará, Mato Grosso, and Rondônia states (Fig. 1), which is consistent with annual rates of NPP estimated by the model across forest types of Brazil (Potter et al., 1998). Our model's predicted geographic distribution of forest biomass across the Legal Amazon

Table 1
Allocation and residence time parameters for major vegetation types, following global cover classes defined by DeFries and Townshend (1994)[a]

Vegetation type	α leaf	α root	α wood	τ leaf	τ root	τ wood
Annual grassland and crops	0.45	0.55	—	1.5	5.0	—
Mixed deciduous forest	0.30	0.25	0.45	1.0	3.0	40
Desert and bare ground	0.25	0.25	0.50	1.5	3.0	50
Semi-arid shrub land	0.25	0.25	0.50	1.5	3.0	50
Savanna and wooded grassland	0.30	0.25	0.45	1.0	5.0	25
Tropical evergreen rain forest	0.25	0.25	0.50	1.5	2.0	25

[a] α is the proportional allocation constant of plant tissue pools; τ is the residence time (in years) of carbon in plant tissue pools. Sources for information on parameter settings include: Cannell (1982), Aber and Melillo (1991), Running and Gower (1991), Redente et al. (1992), Lusk et al. (1997), Terborgh et al. (1997), Guild et al. (1998).

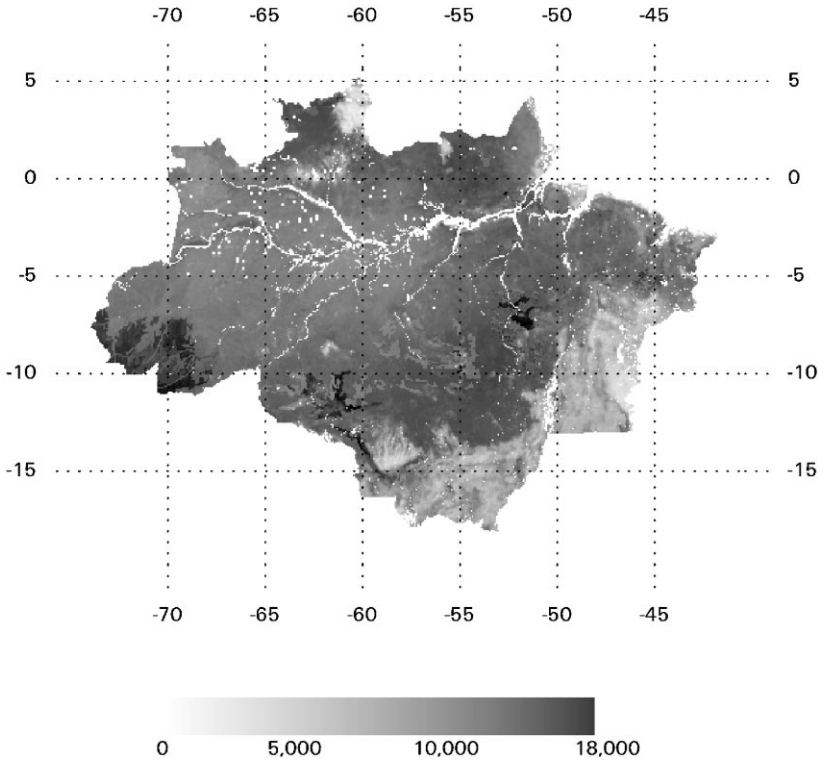

Fig. 1. Regional distribution of aboveground biomass (leaf and wood) estimated from the NASA–CASA model for the early 1990s in states of the Legal Amazon. Units are $g C m^{-2}$.

region differs from that estimated by Houghton et al. (2000), who used stem-wood volume measurements assigned by land cover type or interpolated, mainly in that our model's predicted biomass amounts are relatively higher in the eastern and southern states of the region. The importance of this distinction between estimates of Amazon forest biomass distribution should be noted with respect to the most prevalent locations for deforestation and biomass burning in the region, which are also in the eastern and southern states (Alves, 1999).

3. Satellite data for fire detection

Region-wide fire pixel counts from the AVHRR sensor can be used, in combination with our ecosystem model

results for biomass, for detailed mapping of the daily abundance and spatial distribution of deforestation burning activities in a country like Brazil, provided that these relatively coarse resolution (1-km) satellite data are adjusted for several sources of fire detection bias. Periera et al. (1991), for example, used AVHRR data to evaluate the accuracy of fire detection and burned area estimates in Brazil, and found that all 1-km AVHRR-detected fires had corresponding Landsat TM fire scars, but that actual fire sizes are overestimated by 43%, on average. More recently, Kaufman et al. (1998) reported that the typical size of the hottest areas of fires in Brazil are usually small (e.g., $0.005\,km^2$), with a fire area distribution that peaks at between 0.2 and $1\,km^2$. Hence, while it may be unreasonable to treat AVHRR fire counts as a reliable source for estimating the precise land area burned by fires in the Amazon, for our purposes, 1-km AVHRR fire count data can be used in combination with the NASA–CASA model mainly to detect the location and relative probability of daily biomass burning emissions of carbon to the atmosphere. Additional adjustments and methodology for actual area burned are described in the results that follow.

The most readily available AVHRR fire data set for our analysis is the International Geosphere–Biosphere Programme (IGBP) Global Fire Product (GFP), which provides a consistent data set on daily fire counts at a global scale (Stroppiana et al., 2000; Dwyer et al., 1998; Justice and Dowty, 1993). At this time, the GFP product is available only for an annual period spanning 1992–1993, which closely corresponds to the end of the NASA–CASA simulation period for this study. The GFP fire detection method is based a selection of 1-km pixels that could potentially contain fires, with a confirmation procedure for the fire pixel classification by comparison of the pixel with its immediate geographic neighborhood (Flasse and Ceccato, 1996). The spectral basis for AVHRR fire detection algorithm is channel 3 (3.55–3.93 μm; mid-IR), which is located near the optimum for high radiative emittance typical of vegetation fires (e.g., Langaas and Muirhead, 1988). It is possible to detect fires burning over areas much smaller than the nominal 1-km AVHRR pixel size, because the total radiant emittance from a fire is disproportionally greater than that from a cooler background (Kennedy et al., 1994). Furthermore, there are several noteworthy interference problems with the AVHRR mid-IR signal that must be overcome for accurate fire detection, including surface reflection of solar radiation in the 3.75 μm band, transmission effects of atmospheric water vapor, subresolution clouds, and viewing geometry (i.e., sun-glint effect) of the AVHRR sensor (Gregoire, 1993). Nonetheless, wherever the GFP indicates high fire counts, these pixels should accurately represent cloud-free measurements of daily surface fire activity.

To combine AVHRR fire counts with NASA–CASA's predicted biomass values for the Legal Amazon, we first aggregated the 1-km GFP fire count data to the resolution of our 8-km regional grid. All Amazon fires detected in the GFP record during 1992–1993 were counted in order to capture a full year of daily burning activity at each 8-km pixel location. To next generate a 'nominal' burning emission flux of C from each 8-km grid cell in the Legal Amazon region, we multiplied both leaf biomass C and wood biomass C values, as produced from early 1990s NASA–CASA model simulation, by the number of 1-km fire counts per 8-km cell per day of the 1992–1993 annual period.

These gridded results were subsequently multiplied by a mean estimated combustion fraction of 0.95 for leaf material and a combustion fraction (CF) of 0.45 for wood material, derived from Amazon forest burning studies (Kauffman et al., 1995; Guild et al., 1998; Sorrensen, 2000), to generate maps of the nominal burning emission fluxes of C for 365 consecutive days. We based these estimates for typical CF values on studies that were conducted in the Amazon on small-holder properties, where all decisions as to which vegetation to burn, size of area slashed, location, and the timing of the slash and burn process (how to slash, how long to dry, when to burn) were entirely left to property owners. The initial distribution of biomass among tissue fractions (e.g., wood, leaf) and sizes may help explain differences found in CF values among burning experiments (Fearnside et al., 2000), and the estimated CFs used in our analysis are fairly typical of those reported in several other studies of tropical biomass burning (Hao and Liu, 1994; Graça et al., 2000). This is in contrast to the atypically low CF value of 0.2 used by Houghton et al. (2000) for computing the entire fraction of forest biomass lost during burning events in the Amazon, without regard to different tissue fractions.

It is necessary next to 'scale-down' our nominal burning emission fluxes, which are evidently biased toward area overestimation in 1-km fire counts. An adjustment is required to make areas inferred from the GFP fire counts closely match deforestation area rates reported by the Brazilian Space Agency, INPE, which based its estimates on analysis of Landsat imagery for the 1990s (Alves, 1999). This is accomplished by comparison of the annual (1992–1993) total 1 km fire pixel counts in primary forest areas delineated by Stone et al. (1994) per state of the Legal Amazon to state-by-state INPE deforestation area estimates (reported, for example, in Houghton et al. (2000) and Kaufman et al. (1998)). This comparison generates a set of ratio conversion factors (Table 2), which can then be used to proportionally reduce the nominal burning C emission estimates derived from total 1-km AVHRR fire counts. We find that the region-wide ratio of INPE-estimated area deforested divided by 1-km forest fire count is 0.23.

According to the GFP record for 1992–1993, 75% of all fire counts in the Legal Amazon region were in areas

Table 2
Aboveground biomass, deforestation rates, AVHRR fire counts, and associated carbon emissions for 1992–1993 in States of the Legal Amazon

	Aboveground biomass[a] (pg C)	Rate of deforestion[b] (10^4 km^2 yr^{-1})	AVHRR 1-km fire count (10^4) in primary forest areas[c]	AVHRR 1-km fire count (10^4) in other land cover areas[d]	Ratio of area deforested to fire counts[e]	Carbon fluxes from biomass burning (Pg C yr^{-1})[f]
Acre	2.36	0.048	0.117	0.045	0.41	0.006
Amapa	1.47	0.004	0.069	0.370	0.06	0.008
Amazonas	17.90	0.037	0.308	0.123	0.12	0.006
Maranhao	3.30	0.114	0.973	6.924	0.12	0.253
Mato Grosso	10.86	0.622	1.486	4.313	0.42	0.205
Pará	15.86	0.428	2.807	2.835	0.15	0.138
Rondônia	3.32	0.260	0.604	0.283	0.43	0.033
Roraima	2.49	0.024	0.149	0.462	0.16	0.009
Tocantins	2.19	0.033	0.008	3.852	4.40	0.110
Total for Legal Amazon	59.74	1.490	6.519	19.207	0.23	0.767

[a]From NASA–CASA model, summed over all land cover classes.
[b]From the Brazilian Space Agency, INPE.
[c]Based on GFP (Stroppiana et al., 2000) in areas of the Legal Amazon defined by Stone et al. (1994) as tropical moist forest.
[d]Other land cover classes with the majority of fire counts are cleared forests, secondary forests, and savanna/woodlands, according to land cover classification by Stone et al. (1994).
[e]Computed as [b]divided by[c].
[f]Includes daily burning and post-burning decomposition emissions of carbon.

outside the primary moist forest zone. These areas have cover types delineated by Stone et al. (1994) as mainly (60%) seasonal deciduous woodlands and secondary forests, presumably interspersed with areas of cattle pasture. The remaining 15% of fires detected outside the primary forest zone were chiefly in savanna/woodlands (*cerrado*). Based on previous Landsat image analyses in such areas outside the primary forest zone, we therefore, assumed a ratio conversion factor for the quantity (burned area: l-km fire pixel count) of 0.73 (Setzer and Pereira, 1991) for these cover types.

4. Regional carbon flux estimates

With these adjustments of fire counts to be consistent with 1992–1993 INPE's deforestation area estimates and in burned *cerrado* areas, we calculate the annual direct burning source of gross C emissions in the entire Legal Amazon to be 0.71 Pg C yr^{-1} (Table 2). More than 85% of this total emission flux was mapped to areas outside of moist primary forest areas. The regional distribution of biomass burning emissions shows deforestation and burning emissions to be highest in the states of Maranhao and Tocantins mainly from burning outside of moist forest areas, and in Pará and Mato Grosso with important contributions from primary forest cutting and burning (Fig. 2).

To help close the long-term regional carbon budget, we can also calculate a post-burning decomposition flux of C from each 8-km grid cell on a daily basis. Losses of residual (unburned) plant material are computed using estimated decomposition emission factors of $2.5\times10^{-2}\,d^{-1}$ for leaf residue and $4.57\times10^{-4}\,d^{-1}$ for wood residue, as reported from decomposition rate experiments in Amazon forests (Chambers et al., 2000). At all 8-km grid locations where active fire counts were detected by AVHRR, the area-adjusted amount of residual plant material is added each day to the decomposing pools of unburned leaf and wood biomass, from which post-burning C emissions from cleared forest areas to the atmosphere are computed by the decomposition algorithms. These 1992–1993 post-burning fluxes are predicted to total 0.056 Pg C yr^{-1} for the entire annual decomposition cycle (Fig. 3), with highest sources in the states of Maranhao and Mato Grosso mainly from decomposition of biomass outside of moist forest areas. Although this yearly estimated post-burning flux from

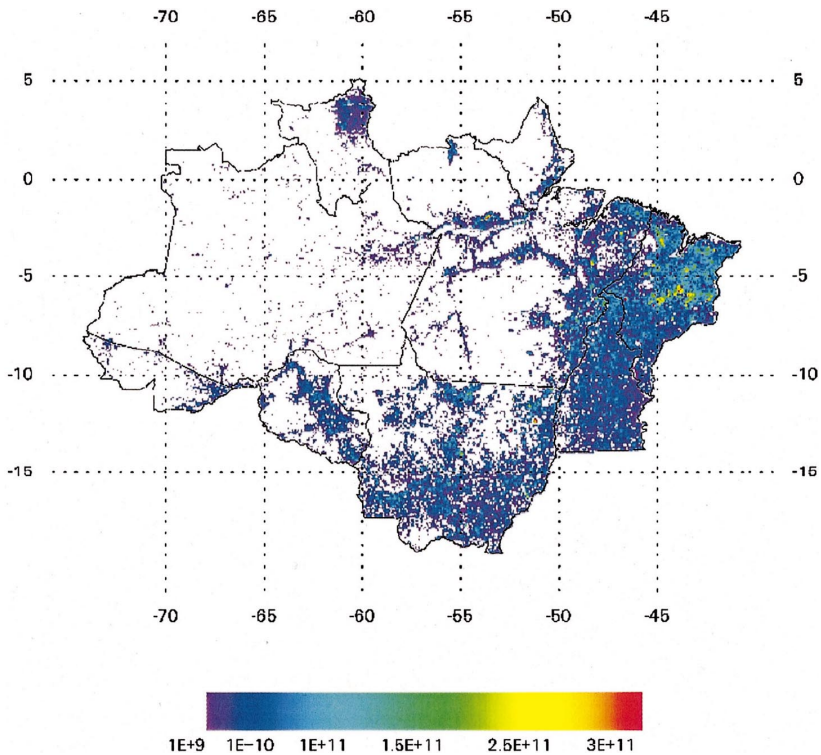

Fig. 2. Regional distribution of total annual (1992–1993) carbon emissions from biomass burning over the Legal Amazon. Includes daily burning and post-burning decomposition emission totals. Units are g C for each 8-km cell.

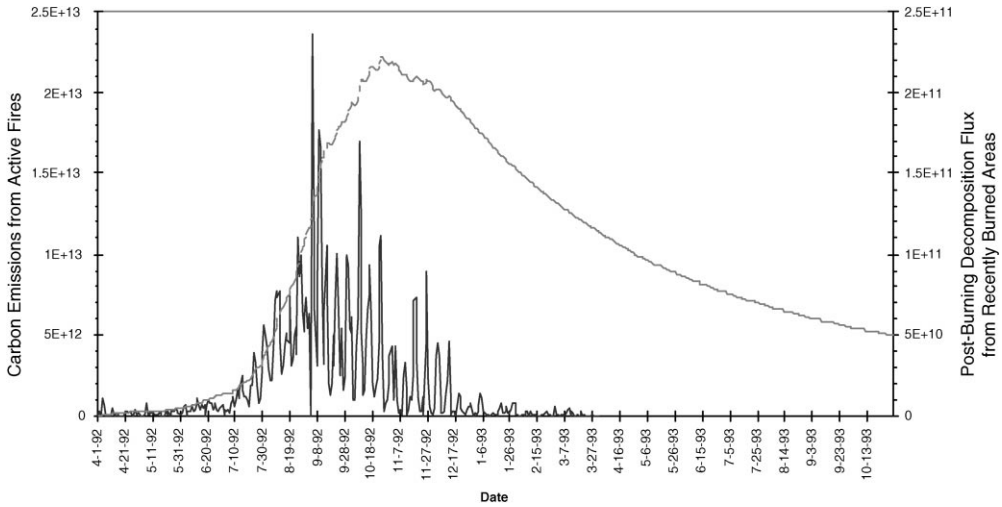

Fig. 3. Carbon emissions resulting from biomass burning by day of the year 1992–1993, summed for the entire Legal Amazon region. Solid line is the daily carbon emission estimate from active fires, Dashed line is post-burning decomposition flux estimate of carbon to the atmosphere from recently burned areas. Units are $g\,C\,d^{-1}$; note different scales for the two emission sources.

our model is less than 10% of direct annual burning emissions for the region, relatively slow rates of decomposition of residual wood pools would extend these post-burn losses of carbon into subsequent annual periods.

The predicted daily flux of carbon to the atmosphere directly from deforestation and biomass burning shows emissions increasing rapidly at the end of July, reaching peak levels in early September and decreasing gradually until mid-December, 1992 (Fig. 3). Post-burning decomposition fluxes of C are logged (with respect to direct burning fluxes) and are carried out in this simulation for six months following the last date of AVHRR fire counts from the GFP record. From this time series, we estimate total gross loss of terrestrial biomass carbon from deforestation and annual burning activities in the Brazilian Legal Amazon for the 1992–1993 period at 0.77 Pg $C\,yr^{-1}$.

This is in contrast to the lower rate of carbon release reported by Houghton et al. (2000) using INPE deforestation estimates at between 0.102 and 0.264 Pg $C\,yr^{-1}$ for the Legal Amazon (forest zones only) in the 1990s. Because INPE's annual estimated rates of deforestation show 1992–1993 as below average compared to all the years of the 1990s, we assume that the 1992–1993 carbon release prediction of Houghton et al. (2000) would be near the low end (i.e., 0.10–0.16 pg $C\,yr^{-1}$) of their reported range of annual emissions for the 1990s. This range for deforestation emissions of carbon is inclusive of our own regional estimate for primary moist forest zones alone of 0.104 pg $C\,yr^{-1}$. Nevertheless, for the reasons stated above relating to assumed CF values, the regional distribution of fires and forest biomass estimates, and extensive coverage of seasonal woodlands, secondary forests, savanna, and pasture vegetation across the region (particularly in the eastern and southern Amazon), we estimate the actual rates of carbon release from deforestation of all kinds and fires over the Legal Amazon were three to five times higher than those computed by Houghton et al. (2000) or by Fearnside (1997). This comparison, albeit with inclusion of different land cover types, is important as a point of clarification, because Houghton et al. (2000) discussed their regional deforestation carbon emission estimates on an equivalent basis with total carbon sink fluxes in all natural (relatively undisturbed) ecosystems of the region, to conclude that the Legal Amazon region is nearly a net-zero source of terrestrial carbon.

5. Concluding remarks

It is important to note that biomass burning fluxes of trace gases alone are not identical to annual net fluxes from land-use change. Biomass burning is a gross emission of carbon, which may be balanced over periods of 25–50 years by uptake of atmospheric carbon during vegetation regrowth, provided that forest burning is not associated with a permanent land-use change. Houghton et al. (2000), for instance, reported average net fluxes of carbon (burning, decomposition, and regrowth) of 0.18 Pg $C\,yr^{-1}$ from Legal Amazon deforestation, but since these investigators conclude that annual sink flux of carbon attributable to secondary forest regrowth is probably not large (<0.15 Pg $C\,yr^{-1}$) compared to potential deforestation CO_2 sources in the region, their net carbon

flux estimates are in fact dominated by gross biomass burning and post-burning decomposition losses to the atmospheric CO_2 pool. Hence, there is no evidence in the literature that gross emissions may be balanced in a single year by large areas of regrowing tropical forests burned in previous years.

The results from this study and related NEP predictions from the NASA–CASA model (Potter et al., 2000) do not support the conclusion of the Legal Amazon as a net-zero annual source for terrestrial carbon fluxes. To adequately address the question of whether any region is a net source or a net sink for carbon during recent years, disturbance related fluxes, like those from deforestation and biomass burning, must be combined with at least 10 years of NEP estimates for relatively undisturbed primary forest ecosystems, in order to understand interannual variability in terrestrial carbon exchange caused in large part by droughts associated with El Niño Southern Oscillations (ENSO) events (Nepstad et al., 1999). Potter et al. (2000) estimated that Legal Amazon NEP varies between $\pm 0.5\,\mathrm{Pg\ C\,yr^{-1}}$, which is in general agreement with previous NEP predictions for the region by Tian et al. (1998). When annual emission fluxes from biomass burning are included for the entire region, our analysis implies that the total net source fluxes from the Brazilian Amazon, including all undisturbed plus disturbed ecosystem classes, can range from 0.7 to $1.2\,\mathrm{Pg\ C\,yr^{-1}}$ during strong ENSO drought years, but can revert to a smaller net source flux of about 0.1–0.2 $\mathrm{Pg\ C\,yr^{-1}}$ during other years when rainfall is not limiting to plant production.

Acknowledgements

We thank Michael Keller and two anonymous reviewers for helpful comments on an earlier version of the manuscript. This work was supported by a grants from NASA programs in Land Surface Hydrology and the Large Scale Biosphere Atmosphere Experiment in Amazonia (LBA-Ecology Component).

References

Aber, J.D., Melillo, J.M., 1991. In: Terrestrial Ecosystems. Saunders College Publishers, Philadelphia, pp. 429.

Agbu, P.A., James, M.E., 1994. NOAA/NASA Pathfinder AVHRR Land Data Set User's Manual. Goddard Distributed Active Archive Center, NASA Goddard Space Flight Center, Greenbelt.

Alves, D.S., 1999. Geographical patterns of deforestation in the 1991–1996 period. Proceedings of the 48th Annual Conference of the Center for Latin American Studies. Patterns and Processes of Land Use and Forest Change in the Amazon. University of Florida, Gainesville, March 23–26.

Bishop, J.K.B., Rossow, W.B., 1991. Spatial and temporal variability of global surface solar irradiance. Journal of Geophysical Research 96, 16839–16858.

Cannel, M.G.R., 1982. World Forest Biomass and Primary Production Data. Academic Press, London.

Chambers, J.Q., Higuchi, N., Schimel, J.P., Ferreira, L.V., Melack, J.M., 2000. Decomposition and carbon cycling of dead trees in tropical forests of the central Amazon. Oecologia 122, 380–388.

Ciais, P., Tans, P.P., White, J.W.C., Trolier, M., Francey, R.J., Berry, J.A., Randall, D.R., Sellers, P.J., Collatz, J.G., Schimel, D.S., 1995. Partitioning of ocean and land uptake of CO_2 as inferred by ^{13}C measurements from the NOAA Climate monitoring and diagnostics laboratory global air sampling network. Journal of Geophysical Research 100, 5051–5070.

DeFries, R., Townshend, J., 1994. NDVI-derived land cover classification at global scales. International Journal of Remote Sensing 15, 3567–3586.

Dwyer, E., Grégoire, J.-M., Malingreau, J.P., 1998. A global analysis of vegetation fires using satellite images: spatial and temporal dynamics. Ambio 27 (3), 175–181.

Fearnside, P.M., Graça, P.M.L.A., Leal Filho, N., Rodrigues, F. J. A., Robinson, J.M., 2000. Tropical forest burning in Brazilian Amazonia: measurements of biomass, burning efficiency and charcoal formation at Altamira, Pará Forest and Ecological Management 123, 65–79.

Fernside, P.M., 1997. Greenhouse gases from deforestation in Brazilian Amazonia: net committed emissions. Climatic Change. 35, 321–360.

Flasse, S.P., Ceccato, P.S., 1996. A contextual algorithm for AVHRR fire detection. International Journal of Remote Sensing 17, 419–424.

Gleeson, S.K., Tilman, D., 1990. Allocation and the transient dynamics of succession on poor soils. Ecology 71, 1144–1155.

Graça, P.M.L.A., Fearnside, P.M., Cerri, C.C., 1999. Burning of Amazonian forest in Ariquemes, Rondônia, Brazil: biomass, charcoal formation and burning efficiency. Forest and Ecological Management 120, 179–191.

Gregoire, J.-M., 1993. Use of AVHRR for the study of vegetation fires in Africa: fire management perspectives. Euro Courses: Advances in the use of AVHRR Data for Land Applications, Ispra, Italy.

Guild, L.S., Kauffman, J.B., Ellingson, L.J., Cummings, D.L., Castro, E.A., 1998. Dynamics associated with total aboveground biomass, C, nutrient pools, and biomass burning of primary forest and pasture in Rondônia, Brazil during SCAR-B. Journal of Geophysical Research 103, 32091–32100.

Hao, W.M., Lui, M.-H., 1994. Spatial and temporal distribution of tropical biomass burning. Global Biogeochemical Cycles 8, 495–503.

Houghton, R.A., Skole, D.L., Nobre, C.A., Hackler, J.L., Lawrence, K.T., Chomentowski, W.H., 2000. Annual fluxes of carbon from deforestation and regrowth in the Brazilian Amazon. Nature 403, 301–304.

Justice, C. O., Dowty, P., 1993. IGBP-DIS satellite fire detection algorithm workshop technical report. IGBP-DIS Working Paper No. 9, NASA/GSFC, Greenbelt, MD, USA, 88pp.

Kauffman, J.B., Cummings, D.L., Ward, D.E., Babbitt, R., 1995. Fire in the Brazilian Amazon: biomass, nutrient pools, and losses in slashed primary forests. Oecologia 104, 397–408.

Kaufman, Y.J., Hobbs, P.V., Kirchhoff, V.W.J.H., Artaxo, P., Remer, L.A., Holben, B.N., King, M.D., Prins, E.M., Ward,

D.E., Longo, K.M., Mattos, L.F., Nobre, C.A., Spinhirne, J.D., Ji, Q., Thompson, A.M., Gleason, J.F., Christopher, S.A., Tsay, S.-C., 1998. Smoke, clouds, and radiation-Brazil (SCAR-B) experiment. Journal of Geophysical Research 103, 31783–31808.

Kennedy, P.J., Belward, A.S., Gregoire, J.-M., 1994. An improved approach to fire monitoring in West Africa using AVHRR data. International Journal of Remote Sensing 15, 2235–2255.

Langaas, S., Muirhead, K., 1988. 'Monitoring' bushfires in west Africa by weather satellite. In: Proceedings of the 22nd International Symposium on Remote Sensing of Environment, Abidjan, Cote d'Ivoire, 20–26 October, Vol. 2. ERIM, Ann Abor, MI, pp. 253–268.

Los, S.O., Justice, C.O., Tucker, C.J., 1994. A global 1×1 NDVI data set for climate studies derived from the GIMMS continental NDVI data. International Journal of Remote Sensing 15, 3493–3518.

Lusk, C.H., Contreras, O., Figueroa, J., 1997. Growth, biomass allocation and plant nitrogen concentration in Chilean temperate rainforest tree seedlings: effects of nutrient availability. Oecologia 109, 49–58.

Ministério das Minas e Energia (MME), 1981. Projeto RADAMBRASIL, Rio De Janeiro, Brazil.

Nepstad, D.C., Veríssimo, A., Alencar, A., Nobre, C., Lima, E., Lefebvre, P., Schlesinger, P., Potter, C., Moutinho, P., Mendoza, E., Cochrane, M., Brooks, V., 1999. Large-scale impoverishment of Amazonian forests by logging and fire. Nature 398, 505–508.

New, M., Hulme, M., Jones, P., 2000. Representing twentieth century space-time climate variability. II. Development of 1901-1996 monthly grids of terrestrial surface climate. Journal of Climate 13, 2217–2234.

Pereira Jr., A. C., Setzer, A. W., dos Santos, J. R., 1991. Fire estimates in savannas of Central Brazil with thermal AVHRR/NOAA Calibrated by TM/Landsat. Presented at the 24th International Symposium on Remote Sensing of Environment, Rio de Janeiro, Brazil, 27–31 May 1991.

Potter, C.S., 1999. Terrestrial biomass and the effects of deforestation on the global carbon cycle. Bioscience 49, 769–778.

Potter, C.S., Davidson, E.A., Klooster, S.A., Nepstad, D.C., de Negreiros, G.H., Brooks, V., 1998. Regional application of an ecosystem production model for studies of biogeochemistry in Brazilian Amazonia. Global Change Biology 4 (3), 315–334.

Potter, C.S., Klooster, S.A., 1997. Global model estimates of carbon and nitrogen storage in litter and soil pools: response to change in vegetation quality and biomass allocation. Tellus 49B (1), 1–17.

Potter, C.S., Klooster, S.A., 1999a. Dynamic global vegetation modeling (DGVM) for prediction of plant functional types and biogenic trace gas fluxes. Global Ecology and Biogeography Letters 8, 473–488.

Potter, C.S., Klooster, S.A., 1999b. Detecting a terrestrial biosphere sink for carbon dioxide: interannual ecosystem modeling for the mid-1980s. Climatic Change 42 (3), 489–503.

Potter, C. S., Klooster, S., de Carvalho, C. R., Brooks-Genovese, V., Torregrosa, A., Dungan, J., Bobo, M., Coughlan, J., 2000. Modeling seasonal and interannual variability in ecosystem carbon cycling for the Brazilian Amazon region. Journal of Geophysical Research (in press).

Potter, C.S., Randerson, J.T., Field, C.B., Matson, P.A., Vitousek, P.M., Mooney, H.A., Klooster, S.A., 1993. Terrestrial ecosystem production: a process model based on global satellite and surface data. Global Biogeochemical Cycles 7 (4), 811–841.

Priestly, C.H.B., Taylor, R.J., 1972. On the assessment of surface heat flux and evaporation using large-scale parameters. Monthly Weather Review 100, 81–92.

Redente, E.F., Friedlander, J.E., McLendon, T., 1992. Response of early and late successional species to nutrient gradients. Plant and Soil 140, 127–135.

Running, S.W., Gower, S.T., 1991. FOREST-BGC, A general model of forest ecosystem processes for regional applications. II. Dynamic carbon allocation and nitrogen budgets. Tree Physiology 9, 147–160.

Sellers, P.J., Tucker, C.J., Collatz, G.J., Los, S.O., Justice, C.O., Dazlich, D.A., Randall, D.A., 1994. A global 1×1 NDVI data set for climate studies. Part 2: the generation of global fields of terrestrial biophysical parameters from the NDVI. International Journal of Remote Sensing 15, 3519–3545.

Setzer, A.W., Pereira Jr., A.C., 1991. Amazon biomass burnings in 1987 and an estimate of their tropospheric emissions. Ambio 20, 19–22.

Sorrensen, C.L., 2000. Linking smallholder land use and fire activity: examining biomass burning in the Brazilian Lower Amazon. Forest and Ecological Management 128, 11–25.

Stone, T.A., Schlesinger, P., Houghton, R.A., Woodwell, G.M., 1994. A map of vegetation of South America based on satellite imagery. Photogrammetric Engineering and Remote Sensing 60, 541–551.

Stroppiana, D., Pinnock, S., Grégoire, J.-M., 2000. The Global Fire Product: daily fire occurrence from April 1992 to December 1993 derived from NOAA-AVHRR data. International Journal of Remote Sensing 21, 1279–1288.

Terborgh, J., Flores, C.N., Mueller, P., Davenport, L., 1997. Estimating the ages of successional stands of tropical trees from growth increments. Journal of Tropical Ecology 14, 833–856.

Tian, et al., 1998. Effect of interannual climate variability on carbon storage in Amazonian ecosystems. Nature 396, 664–667.

Wilson, S.D., Tilman, D., 1991. Components of plant competition along an experimental gradient of nitrogen availability. Ecology 72, 1050–1065.